Predictive 3D modelling of erosion and deposition in ITER with ERO2.0: from beryllium main wall, tungsten divertor to full-tungsten device

A. Eksaeva[a], A. Kirschner[a,*], J. Romazanov[a], S. Brezinsek[a], Ch. Linsmeier[a], F. Maviglia[b], M. Siccinio[b], S. Ciattaglia[b]

[a]Forschungszentrum Jülich GmbH, Institut für Energie- und Klimaforschung - Plasmaphysik, Partner of the Trilateral Euregio Cluster (TEC), 52425 Jülich, Germany
[b]PPP&T Department, EUROfusion Consortium, Boltzmannstr. 2, 85748 Garching, Germany

Abstract

Erosion and deposition is modelled with ERO2.0 for a hypothetical full-tungsten ITER for an ELM-free H-Mode baseline deuterium discharge. A parameter study considering seeding impurities (Ne, Ar, Kr, Xe) at constant percentages (0.05% to 1.0%) of the deuterium ion flux is done while neglecting their radiation cooling and core plasma compatibility. With pure deuterium plasma, tungsten main wall erosion is only due to charge exchange deuterium atoms and self-sputtering and there is only minor tungsten divertor sputtering. With a beryllium main wall, beryllium erosion is due to deuterium ions, charge exchange deuterium neutrals and self-sputtering. For this case, tungsten in the divertor is eroded by beryllium ions and self-sputtering. The simulations for full-tungsten device including seeded impurities leads to significant tungsten erosion in the divertor. In general, tungsten erosion, self-sputtering and deposition increase by factors larger than 50 at the main wall and 5000 in the divertor compared to pure deuterium plasma.

*Corresponding author: tel.: +49 2461 614277, e-mail: a.kirschner@fz-juelich.de (A. Kirschner)

1. Introduction

The erosion, migration and deposition of beryllium (Be) and tungsten (W) in ITER with a beryllium main wall and tungsten divertor has been modelled in detail in the past. For instance, the erosion and deposition pattern of specific blanket modules has been modelled with the 2D LIM code [1] and later on compared with 3D ERO [2] simulations [3]. These studies provided important information with respect to the expected lifetime of blanket modules and long-term tritium retention associated with beryllium deposition. Afterwards, the ERO simulations were refined using, among other things, updated sputtering data and improved shadowing patterns on the blanket module [4]. More recently, ERO2.0 [5] has been developed, which includes the same physics as ERO but is designed based on massive parallelisation and thus - in contrast to ERO - able to handle significantly larger simulation volumes up to the complete coverage of whole devices. In addition, ERO2.0 allows a flexible implementation of two-dimensionally shaped, realistic surface components. ERO2.0 has been benchmarked successfully against experiments, such as the JET-ILW [5, 6].

First predictive beryllium erosion, migration and deposition modelling for ITER with ERO2.0 has been published in [7]. Benchmarking between ERO2.0 and WallDYN simulations [8, 9] for ITER leads to a good agreement. Recently, a sensitivity analysis of ERO2.0 predictions for beryllium erosion and migration in ITER has been presented in [10]. The extrapolation of plasma parameters into the far scrape-off-layer, the impact angle distribution of beryllium and the assumption for the anomalous transport of beryllium have been identified as important components that significantly influence the modelling results.

The current work presents ERO2.0 modelling of erosion, migration and deposition of tungsten in a full-W ITER device. The modelling serves as a first step towards global impurity modelling of a full-W DEMO device. The simulations are carried out on the JURECA supercomputer [11]. The results are compared with the modelling for ITER with beryllium main wall and tungsten divertor. The plasma background, which is a necessary input for ERO2.0, was provided by the ITER organisation and represents a baseline, ELM-free H-Mode deuterium (D) plasma based on 2D SOLPS/OEDGE modelling. It corresponds to 15 MA, 5.3 T and a power of 100 MW crossing the separatrix into the scrape-off-layer (SOL). This results in an outer wall electron temperature T_e of 10 eV, slightly higher T_e at the inner blanket module BM 5 (a selection of blanket modules is marked in the left part of figure 1) and smaller T_e along the lower part of the inner wall. Within the divertor a maximum T_e of about 10 eV in the outer and 5 eV in the inner divertor appear. At the strike points in the divertor the electron temperatures are about 1 -2 eV. The ion temperature T_i is everywhere roughly a factor of two larger than T_e. For these values of the plasma temperature, D ions energies are at the main wall and divertor below the sputtering threshold of W. The mean energy of CX deuterium atoms, however, can reach up to 1000 eV at the outer wall around the midplane, well above the threshold for tungsten sputtering. Everywhere else at the main wall and within the whole divertor, the CX deuterium atoms energies are too low for W sputtering. At most main wall locations, the electron density, n_e, is between 10^{18} and 10^{19} m^{-3} with smaller densities in particular at the lower part of the inner wall. Within the divertor the highest densities occur at the strike points with about $3 \cdot 10^{21}$ m^{-3}. Beyond the extended grid (i.e. the OEDGE extension of the SOLPS grid [12]) applied for the plasma simulation, a constant extrapolation, i.e.

infinite decay length, of the plasma parameters towards the plasma facing components has been assumed. Thus, the plasma impinging the wall may be considered as a worst case scenario. In toroidal direction the plasma is assumed to be constant. The parallel flow velocity within the SOL is extracted from the SOLPS solution, however, it may be underestimated as plasma fluid drifts are not included in the corresponding SOLPS run. A more detailed description of the plasma parameters and magnetic configuration can be found in [7].
Sputtering and reflection is calculated based on SDTrimSP data that takes into account ion impact energy and angular distributions resulting from the electric sheath in case of ions. For CX neutrals the impact energy needed to calculate the sputter yield is taken from the EIRENE output (only average energy as no distribution is available) and the impact angle is assumed to be 60° relative to the surface normal. The latter assumption is somewhat arbitrary but guided by the view that the neutrals have similar impact angles as the ions and in addition assuming a mean impact angle of about 60° for ions. Mean impact of 60° for ions is widely used in plasma-wall interaction modelling codes and also confirmed by special ERO simulations for various conditions [13, 14].
Modelling using the pure D background plasma without seeding impurities will be presented in section 2. The results for full-W and Be wall / W divertor will be compared with each other. In section 3 various seeding impurities are introduced to study their impact on the overall erosion / deposition at the full-W ITER wall. The plasma parameters themselves are kept unchanged, thus plasma cooling effects and increase of the electron density due to radiation and ionisation of the introduced seeded impurities are neglected. It is noted that the plasma background has been simulated with neon seeding to reach semi-detached divertor conditions as described above, however, the resulting flux of neon particles to the wall components is not available from the corresponding background plasma simulations. Finally, in section 4 the effect of a changed magnetic field configuration resulting in modified edge plasma parameters is analysed for the full-W ITER case. This changed configuration is characterised by the narrowest allowed gap between first and second separatrix at the midplane resulting in increased plasma-wall interaction at certain locations, e.g. at the top of the machine.

2. Simulations with pure deuterium plasma

The simulations with the beryllium main wall show that erosion of beryllium is due to deuterium ions, self-sputtering by eroded beryllium and charge exchange (CX) deuterium atoms. Chemical erosion of beryllium by the formation of Be-D molecules is not considered in the modelling. ERO2.0 simulations for JET-ILW have shown that chemical erosion can contribute significantly to the overall Be erosion depending in particular on the surface temperature [5, 6]. Thus, the importance of Be-D formation will be studied in future ERO2.0 simulations for ITER. About 10% of the eroded beryllium particles migrates to the divertor and is deposited there, whereas 90% of sputtered beryllium is deposited at the main chamber modules. In the divertor, tungsten is sputtered by beryllium particles (originating from main wall sputtering) and self-sputtering by eroded tungsten. Sputtering of tungsten due to deuterium ions and CX atoms does not occur as their impact energy within the divertor is smaller than the sputtering threshold. There is no significant transport of sputtered tungsten particles from the divertor towards the main chamber, however, it has to be noted that thermal forces due to parallel ion and electron temperature gradients

are not yet implemented in the ERO2.0 code and thus are neglected in the simulations. It is planned to upgrade the ERO2.0 code to include these forces and to study their effect on the impurity transport, e.g. with respect to tungsten screening in the divertor.
In a D/T instead of pure D plasma also the heavier tritium particles impinging the divertor tiles would not lead to tungsten sputtering if the same plasma parameters are assumed. However, sputtering of Be in the main chamber would be increased roughly by a factor not larger than 1.5.
The left part of figure 1 shows the resulting beryllium net deposition rate at the plasma facing components, where positive values represent net deposition and negative ones net erosion. Whereas the divertor is deposition-dominated with rates of up to $1 \cdot 10^{21}$ Be/m^2/s, at most locations in the main chamber net erosion occurs with maximum rates larger than $1 \cdot 10^{21}$ Be/m^2/s.
With tungsten instead of beryllium main wall the overall wall erosion is largely reduced. Deuterium ions have too small energies to sputter tungsten from the wall whereas wall sputtering is only due to charge exchange deuterium atoms and self-sputtering by sputtered tungsten particles returning to the wall. The erosion mainly occurs at the outer wall with about 60% due to CX neutrals and 40% due to self-sputtering. About 99% of sputtered tungsten particles from the main wall is redeposited on the main wall (including a minor part of 3.5% lost through the equatorial port and 0.5% to gaps between the main wall panels). The remaining amount of 1% flows to the divertor. There is only minor tungsten sputtering in the divertor due to self-sputtering and thus only small tungsten deposition in the divertor. The right part of figure 1 presents the resulting tungsten net deposition for the full-W case. It can be seen that the tungsten erosion/deposition rates are a factor of more than 10,000 smaller than the beryllium erosion/deposition rates for the Be main wall case.
The consideration of a D/T mixture instead of pure D plasma clearly would increase the W sputtering in the main chamber. As example, at 500 eV impact energy and 60° impact angle, the sputtering due to T is about 3 times larger than due to D, and thus sputtering with D/T is about 2 times larger than with pure D - at smaller impact energies this factor is even larger. However, sputtering in the divertor would not be affected significantly.

3. Simulation with various seeding species in the plasma for the full-W wall

While keeping the plasma parameters unchanged, thus ignoring radiative cooling, the different seeding impurities neon (Ne), argon (Ar), krypton (Kr), and xenon (Xe) are added as singly ionised species to the background flux impinging the plasma facing components. For this purpose, percent values of 0.05%, 0.1%, 0.2%, 0.5% and 1% relative to the impinging deuterium ion flux have been assumed. It has to be noted that in particular the highest concentrations for Kr and Xe are not realistic as the core plasma will suffer from radiation collapse - however, here the main focus is on a simple parameter study. As an example figure 2 a) shows the net W deposition rates for the case of 0.2% Ne indicating an overall similar distribution as for the pure deuterium case shown in figure 1. However, with Ne seeding additional areas are now subject of sputtering, e.g. at the inner wall and in particular in the divertor. In the extreme case of 1% seeding with heavier species like Xe or Kr, the overall increase of net W deposition rates compared to pure D plasma is about a factor of 50. Also the rates of W gross erosion and as consequence the W self-sputtering rates at the main wall increase by a factor up to about 50. In all cases there is,

in addition to sputtering caused by CX atoms and self-sputtering, significant W erosion at the main wall due to the seeded impurities. In some cases the erosion is even dominated by seeded impurities. Within the divertor strong W erosion due to the seeded species and resulting self-sputtering occur, whereas for the pure D plasma, divertor W erosion is very small. Figure 3 shows examples of modelled surface-integrated rates for the Ne and Kr seeding cases: W gross and net erosion, W deposition and the W gross erosion due to the seeded species and due to self-sputtering. The rates are presented separately for the blanket and for the divertor. The key results can be summarised as following:

- The gross erosion in almost all cases is dominated by the seeded impurities, which in particular is pronounced in the divertor.
- The net erosion is between ~1% and ~5% of the gross erosion at the blanket and between ~0% and ~2% in the divertor.
- The majority of not-redeposited W at the blanket panels is lost through the equatorial port at the outer main chamber or through gaps between main wall panels and about 1% is transported to the divertor.
- Without seeding impurities, there is net W deposition in the divertor due to W entering from the main chamber.
- With seeding, increased W erosion appears in the divertor resulting in integrated net erosion. Typically between 97% and 100% of particles eroded in the divertor are also deposited there. The small amount of eroded particles not deposited in the divertor is lost through poloidal gaps, there is no significant W transport from the divertor to the main chamber.
- The surface-integrated W gross erosion rates in the divertor are typically larger (up to a factor of ~2.5 for 1% impurity seeding) than the ones at the blanket with the exception of no impurity seeding and Ne seeding at the lowest seeding rates. Due to the smaller deposition fractions in the divertor (as consequence of losses through gaps), the difference between the surface-integrated net erosion rates at the blanket and in the divertor can become even larger, up to about 8 for 1% impurity seeding.

The simulations also reveal the expected larger tungsten erosion with seeded impurities of higher mass. As example, the integrated gross erosion with 1% Kr is about 7 times larger in the main chamber and 6 times larger in the divertor compared to the case with 1% Ne. With 1% Xe in comparison to 1% Ne, this factor is 7 both for blanket and divertor.

4. Simulation with alternative magnetic configuration for full-W wall

To investigate the influence of the magnetic configuration, additional simulations have been done for the full-W case with a plasma background having a reduced distance between the first and second separatrix. The modified magnetic configuration is characterised by a narrowest allowed (with respect to first wall power loads) distance Δr_{sep} between first and second separatrix at the outer midplane, whereas the so far applied configuration has a wide Δr_{sep} in the range of 9 - 11 cm (called "wide Δr_{sep} configuration" hereafter). As before the modified plasma corresponds to an ELM-free H-Mode with 15 MA, 5.3 T and a power of 100 MW across the SOL. The electron and ion temperatures along the outer wall are similar as before. However, at the top of the machine the modified configuration results in locally peaked profiles with maximum $T_{e,i}$ by a factor of four larger than the almost constant values of T_e = 10 eV and T_i = 20 eV at these locations in the

wide Δr_{sep} configuration. Along the inner wall the temperatures $T_{e,i}$ are about a factor of two smaller than within the wide Δr_{sep} configuration. The divertor temperature profiles are more peaked with the modified configuration resulting in about four times higher peak values in comparison to the temperatures in the wide Δr_{sep} configuration. Compared to the wide Δr_{sep} configuration, the electron densities in the modified version are up to a factor of 10 smaller along the inner wall, along the outer wall at most locations similar or up to a factor of 30 smaller. The divertor density profiles of the modified configuration resemble the ones of the wide Δr_{sep} configuration, just the inner profile is slightly shifted and has a steeper decay towards the SOL.
A comparison of the deuterium ion and CX atom fluxes and mean energies along the wall and divertor surfaces for the two magnetic configurations is presented in figure 4. It can be seen that the deuterium ion fluxes along the main wall are up to a factor of about 100 smaller in the modified configuration, whereas in the divertor they are more similar except of the decay towards the SOL in the inner divertor. With the modified configuration, the mean ion energies reach significantly higher values at the top of the machine and also in the divertor with maximum values of about 300 eV at the outer divertor. These are rather high impact energies, however, the resulting heat fluxes at these surfaces are still within the ITER heat load specifications that are used as the boundary condition in OEDGE. The CX deuterium atom flux is at most locations a factor of 10 smaller with the modified configuration. At some locations this factor can be up to 100, however, there are also positions with a larger flux, in particular along the top outer blanket modules. The mean energy of CX atoms is at most locations larger with the modified configuration with values even above 1000 eV, by far large enough for tungsten sputtering. For the wide Δr_{sep} configuration this is only the case for a certain region above the outer midplane with maximum mean energies not larger than 1000 eV.
Figure 2 b) shows the modelled 2D distribution of tungsten net deposition for 0.2% Ne in the plasma for the modified magnetic configuration. Negative values correspond to the net erosion. Compared to the wide Δr_{sep} configuration (figure 2 a)) the net deposition pattern is more spread along the outer wall towards the outer divertor and there are more pronounced affected regions at the top of the machine (not clearly visible in the figure due to colour scaling) and around the midplane at the inner wall. In addition, in contrast to the wide Δr_{sep} case, there is an extended area of positive net deposition at the upper parts of the outer and inner divertor.
In figure 5 the surface-integrated rates of tungsten gross and net erosion, deposition as well as gross erosion due to the seeded impurities and due to the self-sputtering are summarised for the narrow Δr_{sep} case. The rates are shown for the blanket and divertor separately. The main results without seeding species are the following:

- The integrated tungsten gross erosion at the blanket for the modified configuration is about a factor of ten larger than for the wide Δr_{sep} one. For the net erosion this factor is about 6. The larger gross erosion is a consequence of the significantly higher energy of CX neutrals, which even over-compensates the overall smaller CX fluxes in the modified configuration.
- The smaller electron densities in the modified configuration lead to larger transport of eroded tungsten towards the divertor (2% compared to about 1%). However, the losses through the equatorial port and gaps between first wall panels are smaller (0.5%

compared to 4%) whereas the re-deposition of tungsten at the blanket modules is larger (97.5%) than for the wide Δr_{sep} configuration (95%).

- In the divertor and without seeding species the modified magnetic configuration results in about 1500 times larger gross tungsten erosion compared to the wide Δr_{sep} configuration. One has to keep in mind that the tungsten erosion in the divertor with the wide Δr_{sep} configuration is very small and thus the increased energy of D ions with the modified configuration (in particular at the outer divertor with mean energies of up to 300 eV) leads to comparably large erosion. Whereas without seeding the tungsten gross erosion in the divertor with the wide Δr_{sep} configuration is fully dominated by self-sputtering, deuterium ions also contribute in the case of the modified configuration.
- The net tungsten erosion in the divertor without seeding is about 2% of the gross erosion with the modified magnetic configuration. Not-redeposited tungsten is lost in divertor gaps. As discussed before, in the wide Δr_{sep} configuration, the small gross erosion is over-compensated by the tungsten deposition from the main wall erosion leading to net tungsten deposition in the divertor for the modelling without seeding species.

With seeding species, the surface-integrated gross tungsten erosion at the blanket with the modified magnetic configuration only increases by a factor of about two even at the largest assumed concentration of seeding species. This indicates that - in contrast to the wide Δr_{sep} configuration - now the gross erosion at the blanket is for a large part determined by CX neutrals and not by the seeding species. This is confirmed by the according contributions of seeding species and also self-sputtering to the overall integrated gross erosion rates shown in figure 5.
In the divertor, within the modified magnetic configuration the contribution of seeding species to the overall gross erosion is much larger compared to the blanket area, see figure 5. Thus, as for the non-seeding case, the erosion in the divertor is dominated by ions (deuterium ions and in particular seeded ions for the seeding cases) and self-sputtering and not by CX neutrals, which is also obvious from the rates presented in figure 5. For instance, the tungsten gross erosion with 1% Kr is nearly 20 times larger compared to the non-seeding case. As example, the surface-integrated gross erosion in the divertor with 1% Kr is about 5 times larger for the modified compared to the wide Δr_{sep} magnetic configuration. The according net erosion is about 10 times larger for the modified configuration, indicating a bit smaller redeposition and thus larger loss towards divertor gaps compared to the wide Δr_{sep} configuration.

5. Conclusions and discussion

The presented studies serve as a first step to full-W ITER and DEMO tungsten erosion and deposition modelling. The simulations demonstrate the general feasibility of ERO2.0 application to a full-W ITER device. Despite the semi-qualitative character due to a number of simplified assumptions, the results indicate the importance of a detailed knowledge about the impurity fluxes and impact energies to the wall, plasma parameters and magnetic configuration - all these factors influence the gross and net W erosion. With the background plasma assumptions made within the present work one can conclude that significant tungsten sputtering of the main wall due to CX neutrals can be expected in ITER and DEMO, whereas sputtering of the divertor is dominated by seeded impurity ions

and self-sputtering. Self-sputtering also adds a significant contribution to the overall main wall sputtering. The contribution of tungsten main wall sputtering due to seeded impurities strongly depends on the actual conditions, however, it can become the dominating erosion process.

Whereas in the present work the feedback of the introduced seeded impurities on the plasma parameters (like cooling) has been neglected, this is essential for future simulations as this can strongly reduce the tungsten sputtering caused by the seeded impurities. The large seeding concentrations used here for the parameter study are not realistic, e.g. for the heavier species like Kr, larger concentrations than about 0.1% will not be possible due to radiation cooling and resulting core plasma collapse. Moreover, the assumption of a constant percent value and single charge state of seeded impurity fluxes everywhere to the wall is unrealistic as the flux and charge of seeded impurities should depend on the seeding location. Thus, there is the need of self-consistent plasma modelling including the feedback of seeding species on the plasma and the resulting flux, energy and charge state distribution of seeded impurities to the wall. Also, this will lead to a more realistic spatial distribution of the impurities along the wall depending on the seeding locations.

The present modelling does not include thermal forces. Their influence has to be studied in the future also to analyse the possible transport of eroded tungsten from the divertor to the main wall. It has to be noted that the present work makes use of an infinite decay length for the plasma parameters beyond the extended grid in the far SOL approaching the wall. Applying for instance a non-infinite exponential decay length instead of this rather conservative assumption will lead to a reduction of wall gross erosion and redeposition fraction along the wall components, which will increase the relative amount of tungsten transported to the divertor.

The parallel flow from the SOLPS plasma solution used for the ERO2.0 simulations may be underestimated as drifts are not included. ERO2.0 simulations for ITER with Be main wall and imposed higher flow in general reveal an increased transport of eroded Be impurities from the main wall towards the divertor, in particular to the inner one [10]. Detailed study of such effects for the full-W device will be done in the future.

The results of such modelling can be used to estimate the life time of wall components by analysing the net erosion rates. Also, long-term fuel retention in redeposited layers can be analysed with an assumption of typical fuel content in such layers. Dust formation can be estimated by applying certain conversion factors to the gross erosion rates. Coupling of the ERO2.0 code with a core transport module in addition can lead to the calculation of core tungsten concentration. Last but not least it should be mentioned that compared to ideally smooth surfaces assumed here, the effective sputtering yields can be expected to be reduced due to roughness; some discussion can be found in literature e.g. in [15, 16].

References

[1] S. Carpentier et al., J. Nucl. Mat, 415 (2011) S165
[2] A. Kirschner et al., Nucl. Fusion 40 (2000) 989
[3] D. Borodin et al., Phys. Scr. T145 (2011) 014008
[4] D. Borodin et al., Nucl. Mat and Energy 19 (2019) S510

[5] J. Romazanov et al., Phys. Scr. T170 (2017) 014018
[6] J. Romazanov et al., Nucl. Mat. Energy 18 (2019) 331
[7] J. Romazanov et al., Contr. Plasma Phys., 2020;60:e201900149
[8] K. Schmid et al., Nucl. Fusion 55 (2015) 053015
[9] A. Khan et al., Nucl. Mat. Energy 20 (2019) 100674
[10] J. Romazanov et al., Nucl. Mat. Energy 26 (2021) 100904
[11] Jülich Supercomputing Centre. (2018). JURECA: Modular supercomputer at Jülich Supercomputing Centre. Journal of large-scale research facilities, 4, A132. http://dx.doi.org/10.17815/jlsrf-4-121-1
[12] S. Lisgo et al., J. Nucl. Mat. 438 (2013) S580
[13] K. Schmid et al., Nucl. Fusion 50 (2010) 105004
[14] D. Borodin et al., Phys. Scr. T159 (2010) 014057
[15] M. Küstner et al., J. Nucl. Mat. 265 (1999) 22
[16] A. Hakola et al., Phys. Scr. T159 (2014) 014027

Acknowledgements

The work has been performed under the Task Agreement PMI-5.2.6-T020 between Forschungszentrum Jülich and EUROfusion PPP&T Department. This work has been carried out within the framework of the EUROfusion Consortium and has received funding from the Euratom research and training programme 2014-2018 and 2019-2020 under grant agreement No 633053. The views and opinions expressed herein do not necessarily reflect those of the European Commission.
The authors gratefully acknowledge the computing time granted by the JARA Vergabegremium and provided on the JARA Partition part of the supercomputer JURECA at Forschungszentrum Jülich. The authors would like to thank the ITER Organisation IO for providing the plasma background parameters for the ERO2.0 simulations.

Figures

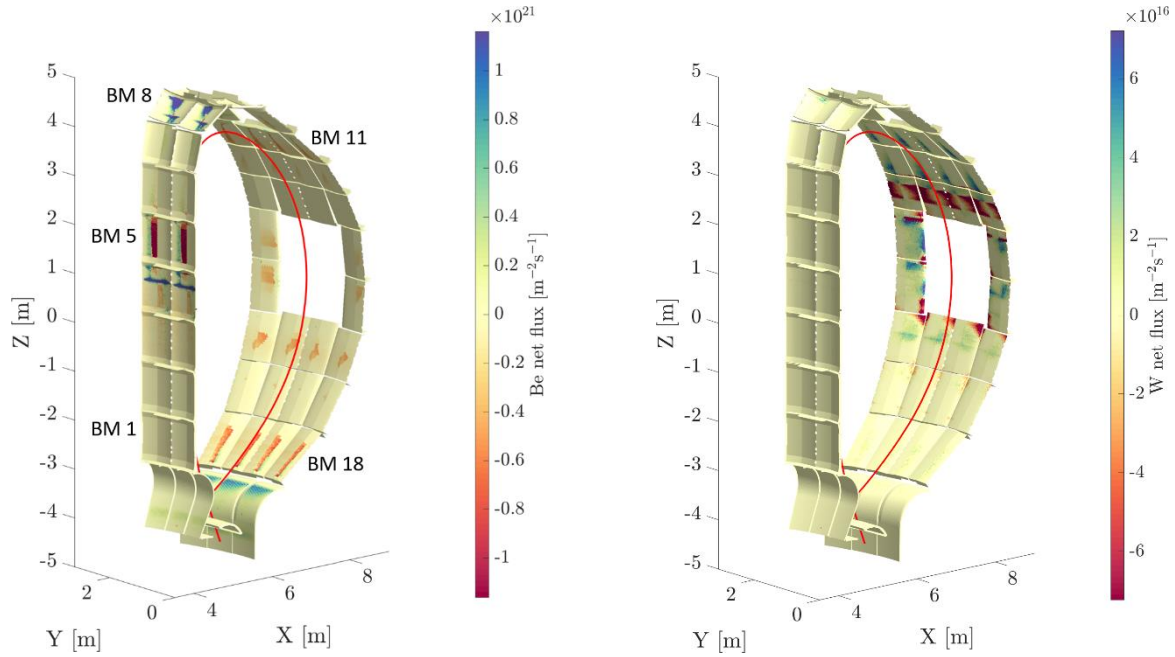

Figure 1 *Modelled net deposition of beryllium for ITER with Be main wall (left) and tungsten for ITER with full-W main wall (right) in pure D plasma without seeding species.*

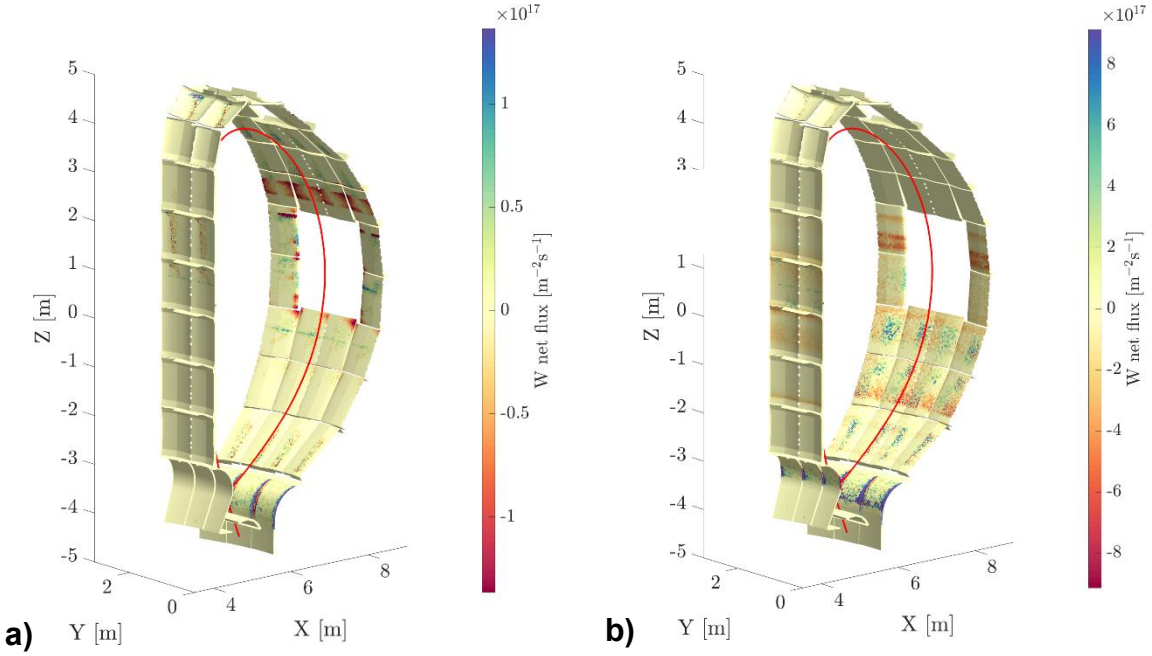

Figure 2 *Modelled tungsten net deposition for full-W ITER including 0.2% Ne in the plasma:* ***a)*** *Magnetic configuration with wide* Δr_{sep} *and* ***b)*** *Modified magnetic configuration with narrow* Δr_{sep}*. Please note that the colour scale has been chosen to illustrate the main features at the outer wall. Therefore, areas of large net erosion at leading edges in the divertor and smaller net erosion/deposition fluxes e.g. at the top of the machine and the inner wall are not visible anymore.*

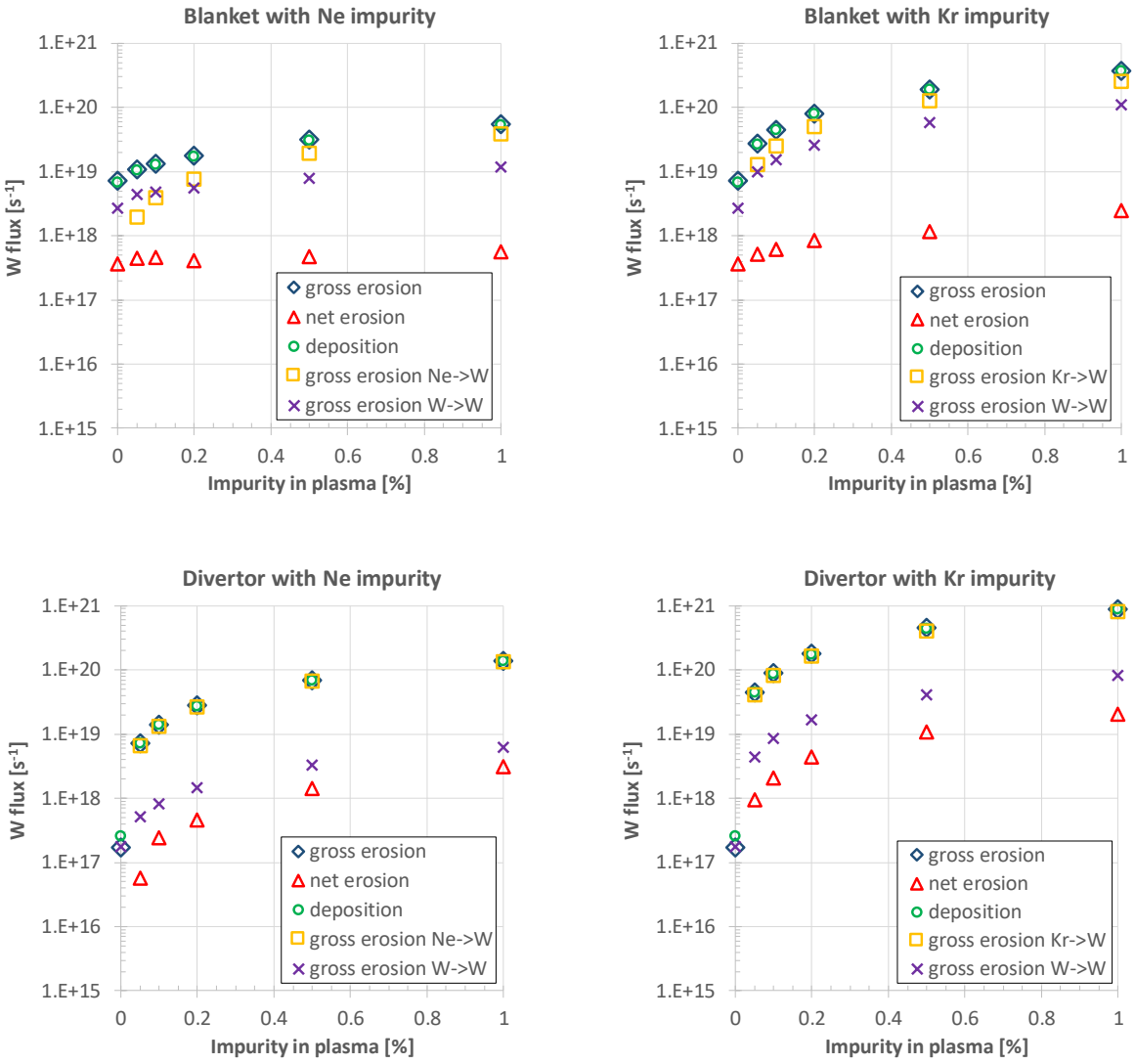

Figure 3 *Surface-integrated rates of W gross and net erosion, W deposition and erosion due to the seeded species and self-sputtering. Left part for Ne seeding, right part for Kr seeding. Upper part for the blanket and lower part for the divertor.*
Please note that the rates of gross erosion and deposition are very close to each other.

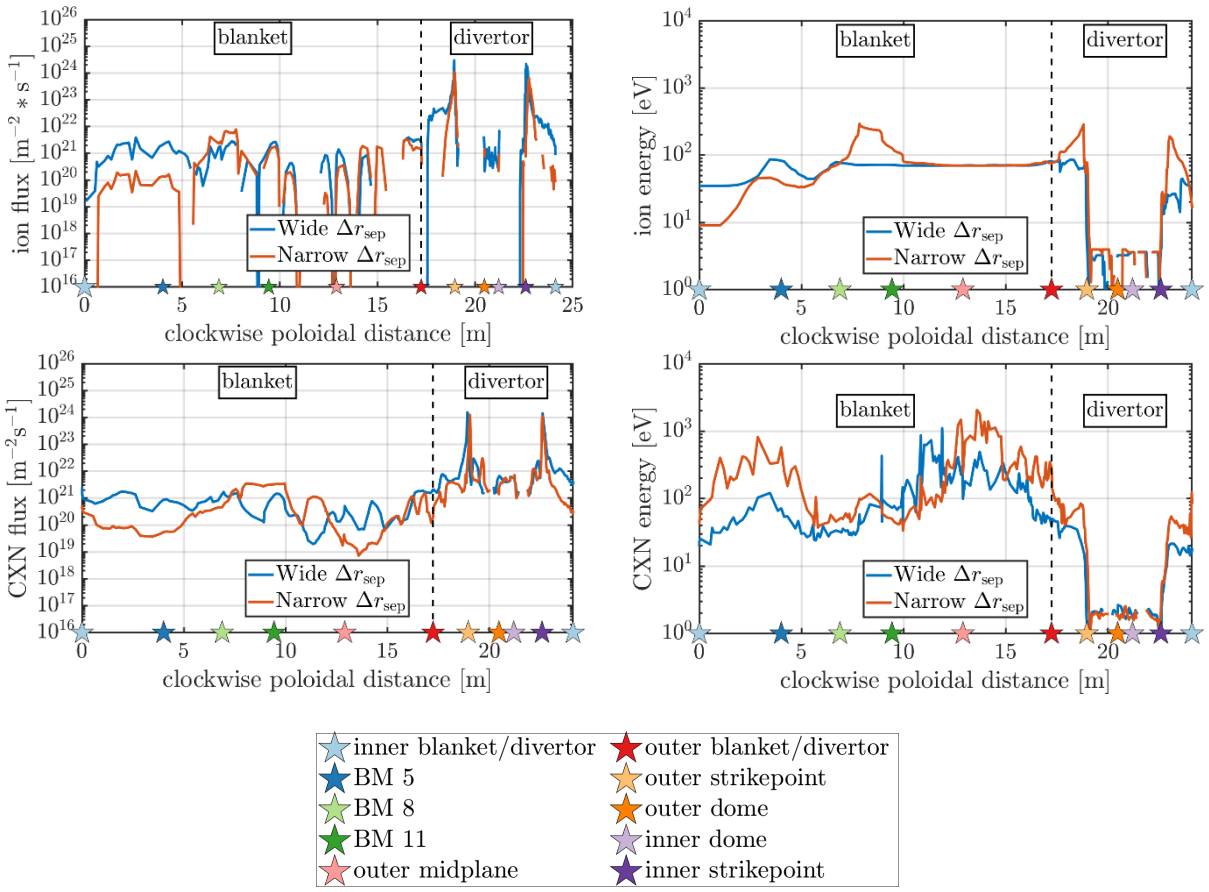

Figure 4 *Deuterium ion flux and mean energy, deuterium CX atom flux and mean energy along the wall and divertor for magnetic configuration with wide Δr_{sep} and modified magnetic configuration with narrow Δr_{sep}. The poloidal distance starts at the end of the inner divertor and terminates thereat. A selection of blanket modules BM is marked in the left part of figure 1.*

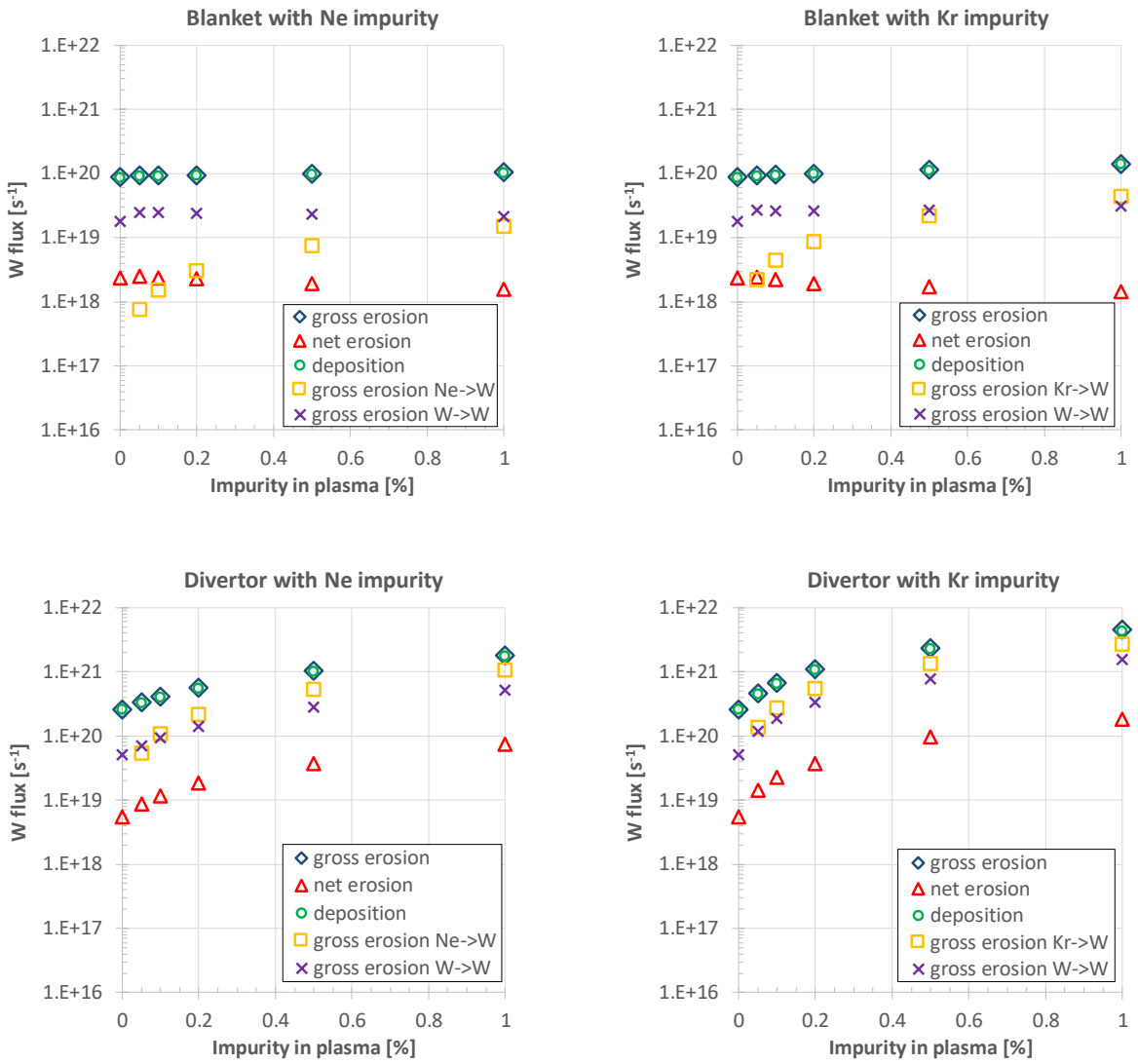

Figure 5 *Modified plasma configuration (narrow Δr_{sep}): surface-integrated rates of W gross and net erosion, W deposition and erosion due to the seeded species and self-sputtering for the. Left part for Ne seeding, right part for Kr seeding. Upper part for the blanket and lower part for the divertor.*
Please note that the rates of gross erosion and deposition are very close to each other.